Journal of The Electrochemical Society, **161** (1) A154-A159 (2014)
0013-4651/2014/161(1)/A154/6/$31.00 © The Electrochemical Society

All-Solid-State Rechargeable Lithium Batteries Using $LiTi_2(PS_4)_3$ Cathode with Li_2S-P_2S_5 Solid Electrolyte

Bum Ryong Shin and Yoon Seok Jung[z]

Interdisciplinary School of Green Energy, Ulsan National Institute of Science and Technology (UNIST), Ulsan 689-798, Korea

The electrochemical performances of $LiTi_2(PS_4)_3$ (LTPS) with a $75Li_2S$-$25P_2S_5$ glass-ceramic solid electrolyte (SE) are investigated. In spite of irreversibility of structural changes, LTPS exhibits a high first discharge capacity of 455 mAh g^{-1} with good cycling retention of 76% at the 25th cycle between 1.5–3.5 V at 50 mA g^{-1} at 30°C. In sharp contrast, LTPS with a liquid electrolyte (LE) in a conventional cell loses half of its initial capacity after only 14 cycles. The much poorer performance of LTPS in the LE compared to that in the SE is believed to be associated with dissolution of LTPS into the LE. The results highlight the prospects of exploring electrode materials that are compatible with SEs for all-solid-state batteries.
 [DOI: 10.1149/2.072401jes]

Manuscript submitted August 29, 2013; revised manuscript received October 11, 2013. Published November 27, 2013.

Demand for safer lithium-ion batteries (LIBs) has been increasing as the application of LIBs has been extended from portable electronic devices to electrified vehicles and energy grids.[1] All-solid-state batteries, where an inorganic solid electrolyte (SE) replaces the flammable liquid electrolyte (LE), have been emerging as one of the most promising next-generation batteries due to their ultimate safety.[2–4] In particular, composite-type all-solid-state batteries where the electrode layer is comprised of active materials, SE powders, and conductive agents have attracted a great deal of attention because of their promise for achieving low process cost and high energy density.[2–6]

Among various candidates for SEs, sulfide-based materials have advantages over other competing oxide materials. Several sulfide SEs with high ionic conductivities on the order of 10^{-3}-10^{-2} S cm^{-1} have been reported: thio-LISICON ($Li_{3.25}Ge_{0.25}P_{0.75}S_4$, 2.2 × 10^{-3} S cm^{-1}),[7] glass-ceramic (GC) $70Li_2S$-$30P_2S_5$ ($Li_7P_3S_{11}$, 3.2 × 10^{-3} S cm^{-1}),[4] LGPS ($Li_{10}GeP_2S_{12}$, 1.2 × 10^{-2} S cm^{-1}).[2] As these sulfide materials are ductile, intimate contact between active materials and SE powders can be easily achieved by a simple cold-pressing procedure.[5,6] One of the critical obstacles to its use, however, is its low oxidation stability.[8,9] Li_2S-P_2S_5 electrolyte shows oxidation onset voltage of ~3.0 V (vs. Li/Li^+).[9,10] In previous reports on layered transition metal oxide cathodes in all-solid-state batteries, interfacial resistance was found to be huge, severely limiting the electrochemical performance.[8,9] It has been reported that this problem can be mitigated by coating the electrode materials with a buffer layer such as $Li_4Ti_5O_{12}$,[11] $LiNbO_3$,[2,12] Li-Si-O,[10] or Al_2O_3.[13]

Another possible approach is to explore alternative electrode materials that operate at mild voltage ranges where the sulfide SEs remain electrochemically stable. Low voltage can be compensated by high capacity if the capacity of the cathode materials is larger than that of the conventional oxide materials. The issue of poor compatibility of electrode materials with LEs can be ruled out in all-solid-state battery systems. Elemental sulfur is one of the promising choices based on the aforementioned considerations. Sulfur has high theoretical capacity ($S + 2Li^+ 2e^- \leftrightarrow Li_2S$, 1672 mAh g^{-1}) and reacts with Li at mild operating voltages (~2.1 V vs. Li/Li^+). Also, the dissolution problem of polysulfide intermediate products into LEs is not a concern for all-solid-state batteries.[14–17] High severe volume change ($\frac{\text{Volume of one mole of } Li_2S}{\text{Volume of one mole of sulfur}}$ = ~179%) during lithiation and delithiation, however, still can limit reversibility of sulfur cathode in all-solid-state batteries.

In this regard, $LiTi_2(PS_4)_3$ (LTPS), which was first reported by Kim et. al.,[1,18,19] is a good candidate for the cathode material in all-solid-state batteries. In a previous report using LEs, LTPS exhibited high capacity (~350 mAh g^{-1} ≡ ~7 Li insertion at first lithiation) and its operating voltage was also mild (<3 V vs. Li/Li^+).[18] Its reversibility, however, was very poor, which was ascribed largely to its structural irreversibility.[19] Incompatibility of LTPS with the LE or dissolution of LTPS is also suspected as the origin of poor performance.[1]

In this report, LTPS is reinvestigated using $75Li_2S$-$25P_2S_5$ GC SE in all-solid-state cells. Structural changes and electrochemical performance of LTPS are examined. More importantly, the performances of LTPS in all-solid-state cells and in conventional LE cells are comparatively discussed. The results reveal that LTPS is dissolved in the LE while LTPS is compatible with the SE, resulting in much better cycling performance with SE than with LE.

Experimental

Preparation of LTPS.— The $LiTi_2(PS_4)_3$ powders were prepared by following the previous reports.[19] Stoichiometric amounts of Li_2S (Alfa Aesar, 99.9%), TiS_2 (Aldrich, 99.8%), and P_2S_5 (Aldrich, 99%) powders were mixed, pelletized under 370 MPa, and put into a carbon-coated quartz tube inside an Ar-filled dry box. The tube was then sealed under vacuum (≤40 Pa). The sealed tube containing the mixture pellet was heat-treated at 750°C for 10 h and subsequently cooled to 400°C at -0.6°C min^{-1}, followed by air-quenching.

All-solid-state cells.— $75Li_2S$-$25P_2S_5$ GC SE powders were prepared by mechanical milling and subsequent heat-treatment. 2 g of batches of Li_2S and P_2S_5 mixture were mechanically milled at 500 rpm for 10 h at room temperature using a planetary ball mill (Pulverisette 7PL; Fritsch GmbH) with a ZrO_2 vial (80 mL) and 115 g of ZrO_2 balls (5 mm in diameter). The obtained glass powders were put into a glass ampoule and sealed under vacuum (≤40 Pa). The sealed ampoule was subjected to heat-treatment at 243°C for 1 h. From electrochemical impedance spectroscopy (EIS) signals collected using 200 mg of $75Li_2S$-$25P_2S_5$ GC SE layer pressed between two Ti rods under 370 MPa for 5 min, ~9.0×10^{-4} S cm^{-1} of electrical conductivity at 30°C was obtained. LTPS composite electrodes were prepared by mixing the LTPS powders, SE powders, and conductive carbon (super P) (20:30:3 wt ratio). 100 mg of a partially lithiated indium ($Li_{0.5}In$, nominal composition) powders prepared by mechanically milling the mixture of In (Aldrich, 99%) and Li (FMC Lithium corp.) powders were used as counter and reference electrode. A SE pellet were formed by pressing 200 mg of $75Li_2S$-$25P_2S_5$ GC SE under 74 MPa. 5 mg of the LTPS composite materials was then carefully spread on the top of the SE layer and the cell was pelletized by pressing under 370 MPa for 3 min. Finally, 100 mg of the prepared $Li_{0.5}In$ powders were attached to the back SE face under 370 MPa. All pressings were carried out in a polyaryletheretherketone (PEEK) mold (diameter = 1.3 cm) with Ti metal rods as current collectors for both working and counter/reference electrodes. All the processes for preparing the SEs and fabricating the all-solid-state cells were performed in the Ar-filled dry box. The galvanostatic discharge-charge cycling of the all-solid-state cells were performed at 50 mA g^{-1} at 30°C and at 100 mA g^{-1} at 60°C. The capacity in this report is based on the

[z]E-mail: ysjung@unist.ac.kr

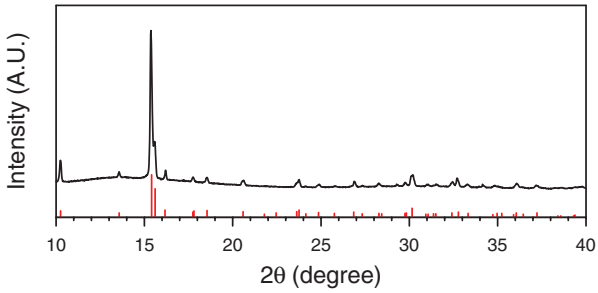

Figure 1. XRD pattern of as-prepared $LiTi_2(PS_4)_3$ powders. The reference peak (JCPDS no. 49–1608) is given at the bottom.

weight of LTPS. The electrochemical impedance spectroscopy (EIS) study was performed using an Iviumstat (IVIUM Technologies Corp.). The AC impedance measurements were recorded using a signal with an amplitude of 10 mV and a frequency range from 500 kHz to 5 mHz. At the targeted cycle for the measurements, the cells were discharged to 1.8 V (vs. Li/Li^+) at 50 mA g^{-1} and the constant voltage of 1.8 V was applied until the current is decreased to 10 mA g^{-1}. Then, the cell was at rest for ≥3 h.

Liquid electrolyte (LE) cells.— A two-electrode 2032-type coin cell was employed to assess the electrochemical performance of the LE cells. A composite electrode was prepared by spreading a slurry mixture of LTPS, super P, and poly(vinylidine fluoride) (PVDF) (70:10:20 wt ratio) on a piece of Al foil. Li metal foil (Alfa Aesar) was used as the counter electrode. 1.0 *M* $LiPF_6$ dissolved in a mixture of ethylene carbonate (EC), diethylcarbonate (DEC) and dimethylcarbonate (DMC) (3:4:3 v/v/v) was used as the electrolyte. Porous 20 μm thick polyethylene (PE) film was used as the separator. All the processes for fabricating the composite electrode and assembling the coin cells were carried out in the Ar-filled dry box.

Materials characterization.— For the XRD analysis, a specially designed cell where the air-sensitive LTPS powders or a disassembled all-solid-state cell pellets were put on a beryllium window and hermetically sealed inside the Ar-filled dry box. Then, the XRD cell was mounted on a D8-Bruker Advance diffractometer equipped with a Cu K_α radiation (1.54056 Å). All the XRD patterns were recorded at 40 kV and 40 mA using a continuous scanning mode with 1.5 deg min^{-1}. The dissolution of sulfur from the LTPS powders and the electrodes into the LE solution was measured by inductively coupled plasma optical emission spectroscopy (ICP-OES) (720-ES, Varian, USA). 1.0 mg of the LTPS powders and the electrodes containing ~0.4 mg of LTPS were put into 5 mL of LE. Then, the LTPS powders in LE and the electrodes in LE were kept at designated temperatures over 10 days. The LE used for the dissolution measurement was the same as the one used for the cycle test in the LE cells.

Results and Discussion

$LiTi_2(PS_4)_3$ powders were synthesized successfully, as indicated by the XRD pattern in Figure 1, where the peaks correspond well with $NaTi_2(PS_4)_3$ (JCPDS no. 49–1680). The pattern also corresponds well with previous results.[18,19]

Figure 2 exhibits SEM images of as-prepared $75Li_2S$-$25P_2S_5$ GC SE powders, LTPS powders, and the electrode. Both SE (Fig. 2a) and LTPS (Fig. 2b) powders have irregular morphology with a few to tens of μm size. As seen in Fig. 2c, the electrode made by pelletizing mixture of LTPS, SE, and carbon additives (20:30:3 wt) exhibits flat surface where the particles are seen to be dented and merged. This observation should be attributed to the ductility of sulfide compounds, both SE and LTPS,[5,6] which makes intimate contact for good ionic conduction pathways. Also the EDS elemental signal of carbon

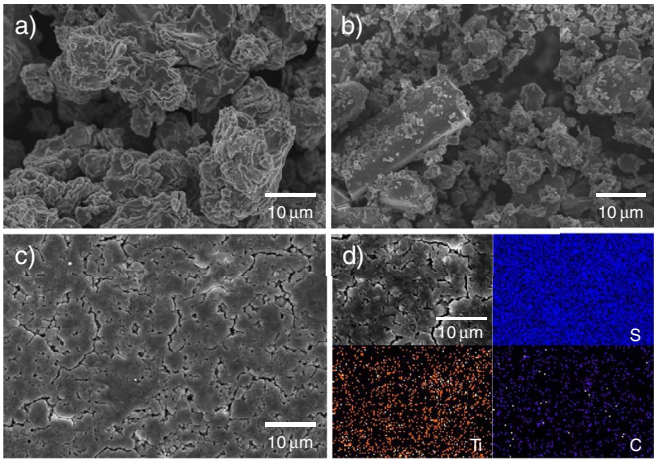

Figure 2. SEM images of a) SE powders, b) LTPS powders, and c) electrode made by pelletizing mixture of LTPS, SE, and carbon additives (20:30:3 wt ratio). d) EDS elemental signals of sulfur, Ti, and carbon of the electrode.

(Fig. 2d) is homogenously distributed, ensuring favorable electronic pathways.

The LTPS electrodes were examined in all-solid-state cells where $75Li_2S$-$25P_2S_5$ GC was used as the SE. The first two lithiation-delithiation voltage profiles of LTPS at 50 mA g^{-1} at 30°C in three different voltage ranges are represented in Fig. 3. For 1.5–3.5 V (Fig. 3a), the LTPS exhibits a first lithiation (discharge) capacity of 455 mAh g^{-1}, which corresponds with insertion of ~10 Li per $LiTi_2(PS_4)_3$. This value is larger than a previously reported result (~7 Li, ~350 mAh g^{-1}) using a conventional LE cell (~3 Li, ~140 mAh g^{-1}).[19] The amount of Li inserted at plateaus at ~2.1 V in Figs. 3a, 3c, and 3d is observed to fall between two and three. Considering the operating voltage for $TiS_2 + Li^+ + e^- \leftrightarrow LiTiS_2$ is ~2.2 V, the reaction at the ~2.1 V plateau of LTPS can be assigned to be reduction of Ti^{4+} to Ti^{3+}.[20,21] A slight excess of inserted Li may be associated with the occurrence of an irreversible reaction, mostly on the surface of carbon additives. In a previous report, it was suggested that 7 Li can be inserted down to 1.5 V, possibly by the reduction of Ti^{4+} to Ti^{2+} and PS_4^{3-} to PS_4^{4-}.[19] On a similar basis, ~10 Li insertion may be explained by the reduction of Ti^{4+} to Ti^{2+} and uptake of two electrons in PS_4^{3-}, which may induce structural reorganization. A possible alternative explanation is the reduction of Ti^{4+} to Ti^+ and uptake of one electron in PS_4^{3-}, which can account for 9 Li per formula unit.[18] The first discharge capacities obtained with the SE were similar to those with the LE in this work, which is discussed later.

The first delithiation from 1.5 V in Fig. 3a results in overall deinsertion of ~11 Li, which indicates that one Li that is initially present in LTPS can be extracted electrochemically as well. In order to confirm this, the LTPS electrode was subjected to delithiation first, as seen in Fig. 3b. Consistent with the results in Fig. 3a, it is shown that the lithium ion in $LiTi_2(PS_4)_3$ is extracted. The second lithiation-delithiation voltage profiles are fairly similar to the first profiles. The second lithiation voltage profile, however, loses the plateau-like features and is smoothened, which is indicative of irreversible structural change. As seen in Fig. 4, the LTPS in 1.5–3.5 V in all-solid-state cells exhibits reasonably good cycling performance (76% of capacity retention at the 25th cycle). This observation is contradictory to previous reports based on conventional LE cells,[19] and highlights prospects of all-solid-state batteries. A detailed discussion on a comparative analysis between SE and LE cells is provided later.

As the lower cutoff voltage decreases from 1.5 V to 1.2 V (Fig. 3c) and 1.0 V (Fig. 3d), the reversibility becomes much poorer. As the lower cutoff voltage is decreased, the discharge-charge voltage profiles change significantly. In particular, the hysteresis between lithiation and delithiation voltage profiles is huge ($\Delta V = \sim 1.8$ V), which

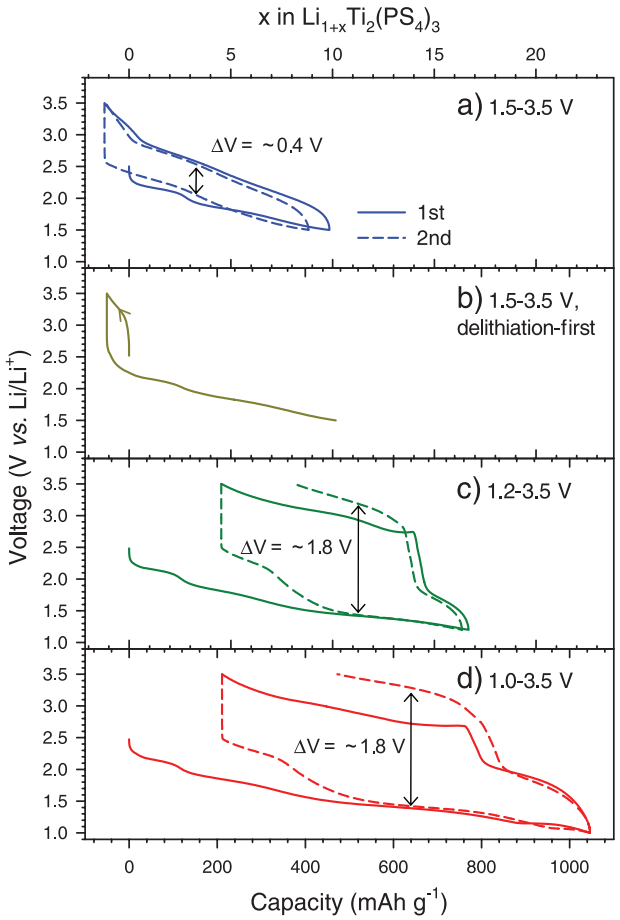

Figure 3. First two discharge-charge voltage profiles of LTPS in all-solid-state cells between a-b) 1.5–3.5 V, c) 1.2–3.5 V, and d) 1.0–3.5 V at 50 mA g^{-1} at 30°C. Charging (or delithiation) was carried out first in b. All the scales are the same.

is one of the typical characteristics of a conversion-type reaction.[22–25] Surprisingly, the amount of Li inserted in $LiTi_2(PS_4)_3$ down to 1.0 V is ~23 Li, which is a much higher value than a previously reported result (~11 Li).[19] The large deviation from the previous result may be associated with the electrode performance of LTPS strongly dependent on the compatibility with the electrolyte. By a naive approach,

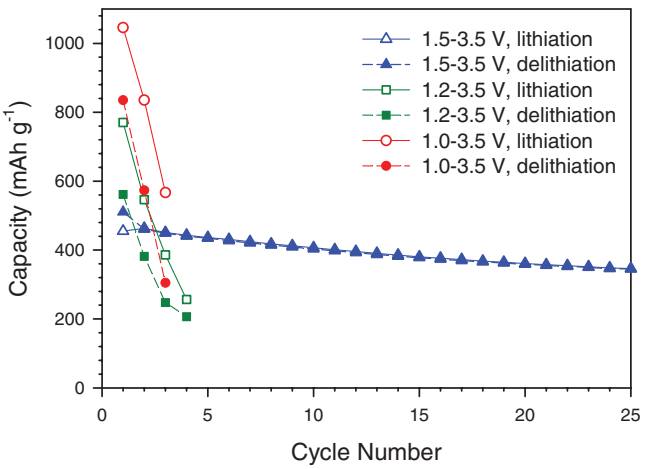

Figure 4. Discharge-charge cycling performance of LPTS in all-solid-state cells in three different voltage ranges at 50 mA g^{-1} at 30°C.

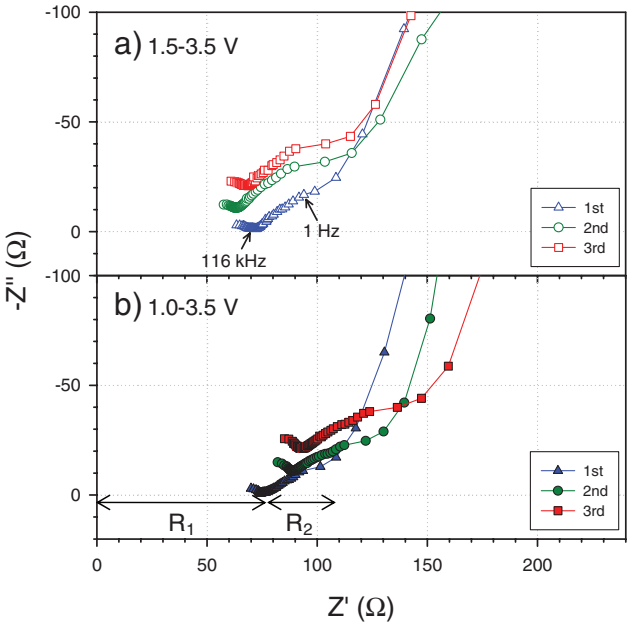

Figure 5. Nyquist plots of LTPS in all-solid-state cells for the first three cycles a) in 1.5–3.5 V and b) in 1.0–3.5 V. The R terms are explained in the main text. The spectra were shifted along the imaginary number axis for clarity.

it can be postulated that, 6 Li may be inserted by reduction of Ti^{4+} to Ti^+ and uptake of more than five electrons of PS_4^{3-}. In this case, complete decomposition of the PS_4^{3-} tetrahedra and thus the formation of Li_2S should follow. Although the capacities are higher with decreased values of the lower cutoff voltage, the cycling stabilities are very poor, as seen in Fig. 4.

The impedance signals of the LTPS/SE/Li-In cells cycled in two different voltage ranges were measured as seen in the Nyquist plots in Fig. 5. The cells at the targeted cycle were discharged to 1.8 V (vs. Li/Li^+). The EIS spectra is comprised of three parts. The first resistance, R_1, is equivalent to the resistance of the SE. This value agrees perfectly with the one obtained from the Ti/SE/Ti cell that is used for the conductivity measurement of the SE. The second resistance, R_2, is attributed to the charge transfer resistance from LTPS/SE and Li-In/SE interfaces.[10] The sloping tails at low frequency are assigned as Warburg term related to Li^+ diffusion in LTPS.[26] In the 1.5–3.5 V, the change of EIS signals on cycling is negligible. In 1.0–3.5 V, in sharp contrast, R_1 is increased after first cycle and, more importantly, the magnitude of the semicircle for R_2 is significantly increased on cycling. These behaviors are in line with the much poorer cycling performance of the LTPS cell in 1.0–3.5 V than in 1.5–3.5 V as seen in Fig. 4. The increases of the resistances in 1.0–3.5 V can be related to loosened contacts between particles and or irreversibility of the electrochemical reaction on repeated cycling.[27]

In an attempt to obtain information on the structural and electrochemical relationships, ex-situ XRD experiments were carried out for LTPS electrodes lithiated and or delithiated at various voltages in all-solid-state cells, and the results are shown in Fig. 6. Most of the results are consistent with previous data.[19] Insertion of Li down to 1.5 V leads to evolution of a new peak at 14.2° ('&'), which is considered as a more-lithiated $Li_{1+a}Ti_2P_3S_{12}$ phase with full consumption of the main LTPS peak at 15.2° ('#'). Delithiation from 1.5 V to 3.5 V results in disappearance of the $Li_{1+a}Ti_2P_3S_{12}$ and evolution of a weak peak at 15.4°. Considering the similar position to the main LTPS peak, the peak at 15.4° likely arises from a delithiated $Ti_2P_3S_{12}$ with a similar structure to that of LTPS. However, the significant decrease of the intensity after a cycle indicates amorphization and irreversibility of the structural changes, which is in line with the slightly changed discharge voltage profile at the second cycle in Fig. 3a. Delithiation to 3.5 V in the range of 1.5–3.5 V at fifth cycle results in a slightly

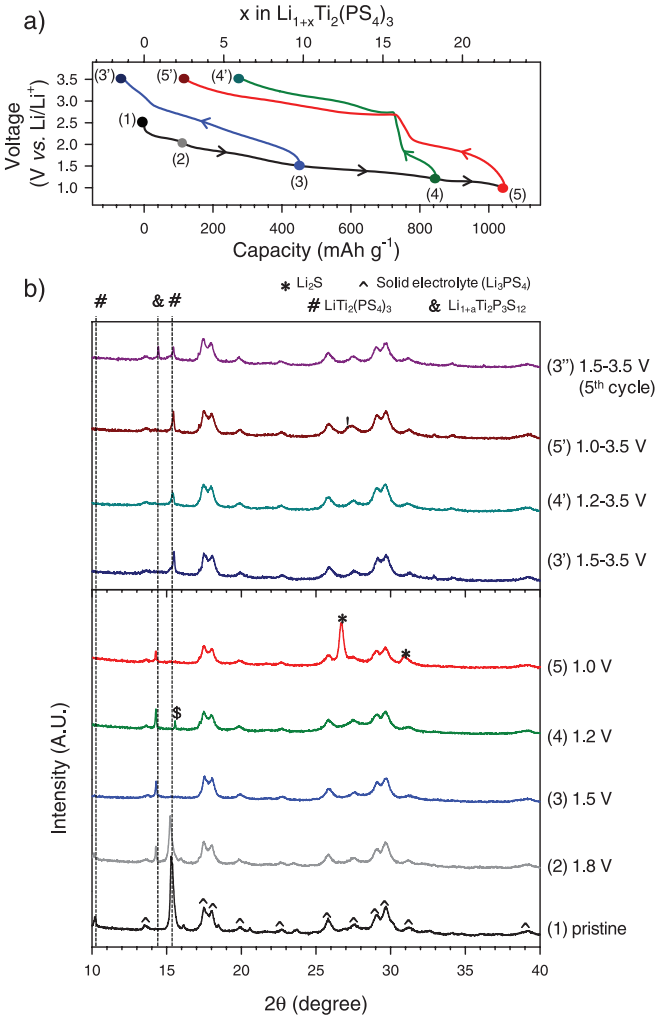

Figure 6. a) First discharge-charge voltage profiles of LTPS in all-solid-state cells at 50 mA g^{-1} at 30°C for ex-situ XRD measurements. b) Ex-situ XRD patterns of LTPS electrode in all-solid-state cells at different discharged and charged states.

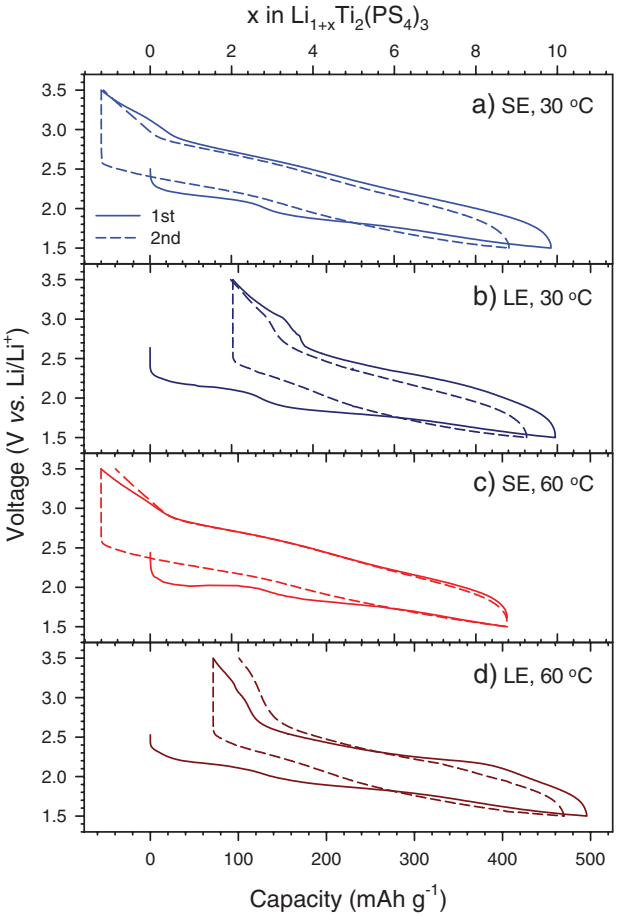

Figure 7. First two discharge-charge voltage profiles of LTPS a) with solid electrolyte (SE) at 30°C, b) with liquid electrolyte (LE) at 30°C, c) with SE at 60°C, and d) with LE at 60°C. The current density at 30°C and 60°C was at 50 mA g^{-1} and 100 mA g^{-1}, respectively.

different pattern (3″) from the first delithiation one (3′). One additional peak corresponding with the lithiated $Li_{1+a}Ti_2P_3S_{12}$ is seen. This observation suggests incomplete delihiation of LTPS after several discharge-charge cycling. Lithiation down to 1.2 V leads to evolution of an unknown peak ('$') at 15.6°. Continuing lithiation down to 1.0 V results in consumption of the $Li_{1+a}Ti_2P_3S_{12}$ peak ('&') and finally evolution of Li_2S ('*'). This result is direct evidence of the conversion reaction of LTPS, which supports the explanation of complete decomposition of PS_4^{3-}. It is interesting that a very weak peak at ~15.4° appears after the delithiation regardless of the lower cutoff voltage. This observation may imply that the delithiated structures from different lower cutoff voltages are similar regardless of whether the LTPS experiences full conversion. The structural changes, however, appear to be very complicated in that there is an additional unknown peak at 27° ('!') in the case of delithiation from the full lithiated state at 1.0 V. One possible explanation on much poorer performances in case that the lower cutoff voltages are under 1.5 V in Fig. 4 may be associated with severer volume changes which is very common in the conversion-type electrode materials.[22–25] As another possible failure mechanism, possible irreversible evolution of some unknown phase should not be ruled out. Because the XRD analysis alone cannot fully elucidate the complex reactions of LTPS, further rigorous analysis using complementary techniques such as X-ray absorption spectroscopy is required.

Recalling that the motivation of this work is that LTPS may be more compatible with a SE than a LE, the electrochemical performances of LTPS are compared between the all-solid-state cells and the conventional LE cells. Fig. 7 represents the first two lithiation-delithiation profiles of LTPS with SE and LE between 1.5–3.5 V at 30°C and 60°C. The current densities at 30°C and at 60°C were 50 mA g^{-1} and 100 mA g^{-1}, respectively. At 30°C, the LE cell shows almost the same first lithiation capacity as that of the SE cell, which supports the reliability of the amount of inserted Li (~10 Li). At elevated temperature (60°C), the cells exhibit roughly similar capacities to those at 30°C. The relatively larger lithiation capacity of the LE cell at first cycle may be associated with side reactions between LTPS and LE.

Fig. 8 compares the cycling behaviors between the SE cells and LE cells at 30°C and 60°C. The voltage range was restricted between 1.5–3.5 V, where the cycling performance with SE is relatively stable. The LE cells show much poorer cycle retention than that of the SE cells. In particular, the LE cell at 60°C loses half of its initial capacity at the 6th cycle. In sharp contrast, the SE cell at 30°C and 60°C retains 76% and 72% of its initial capacities at the 25th cycle, respectively. Considering that the voltage window of 1.5–3.5 V is within the generally accepted stable electrochemical window of the conventional carbonate-based LEs, unfavorable decomposition of the LE can be ruled out as the cause of the poor cycling performance.[1,28,29] As another degradation mode, dissolution of LTPS is strongly suspected.[1] 1.0 mg of the LTPS powder was put into 5 mL of the LE and kept at 60°C for 10 days. The color turned dark red, as indicated by arrow in Fig. 9, suggesting the occurrence of severe dissolution or a side

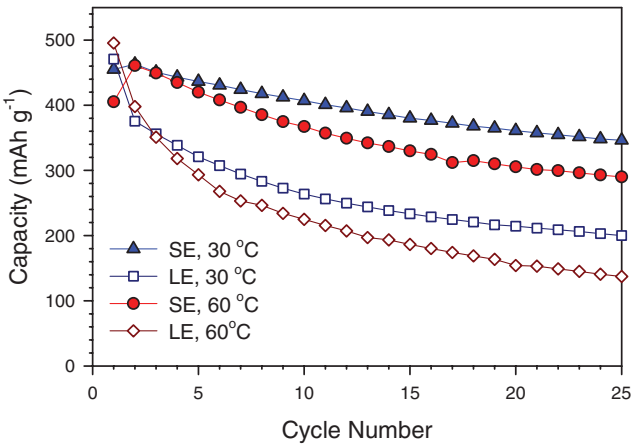

Figure 8. Charge cycling performance of LTPS with SE and LE at two different temperatures (30°C and 60°C).

reaction between LTPS and LE. Table I summarizes the amount of dissolved sulfur and titanium from LTPS into LE after storing pristine LTPS powders and LTPS electrodes in the LE at 30°C and 60°C for 10 days. In all cases, significant dissolution of sulfur took place. At 60°C, in particular, dissolved sulfur to LTPS exceeded 10 wt%. Given this finding, the poorer cycling performance of LTPS with LEs as compared to that with SEs in Fig. 7 and 8 is not surprising. Also the poorer cycling performance of LTPS in LEs at 60°C than at 30°C can be explained by severer dissolution at elevated temperatures. M. Nagao, et al., reported that a poor cyclability observed in Chevrel-phase $Cu_xMo_6S_{8-y}$ electrode in all-solid-state lithium batteries at high temperature is related with diffusion of Cu into the Li_2S-P_2S_5 SE.[30] The slightly inferior capacity retention of LTPS in the SE cell at 60°C to that at 30°C in Fig. 8 may be explained by solid-state diffusion between LTPS and SE on a similar basis.

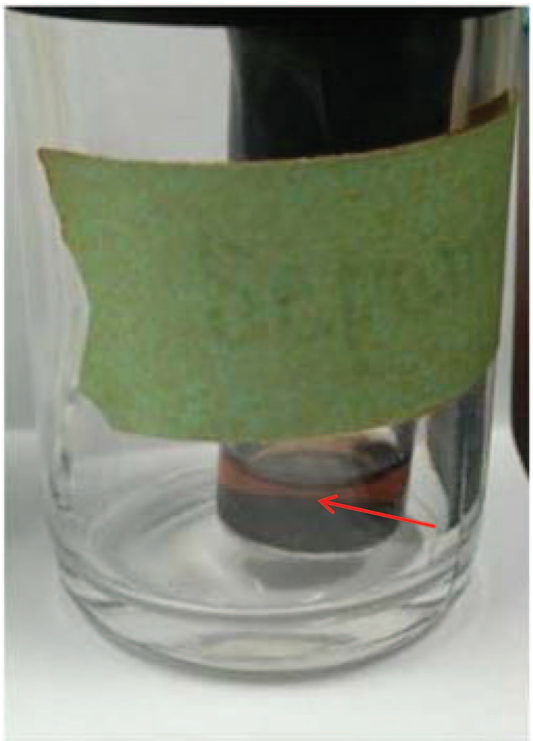

Figure 9. Photograph of LE containing LTPS powders after being kept at 60°C for 10 days. The closed vial was put in the larger glass jar for double-sealing.

Table I. Dissolved amount of sulfur and titanium in liquid electrolyte obtained by ICP-OES measurements.

Sample	Dissolved species	Dissolved amount (%)[a] 30°C	60°C
Powders	Sulfur	-	25.0
	Titanium		0.0
Electrodes	Sulfur	2.1	16.3[b]
	Titanium	0.6	3.1

[a]Weight fraction of the species to LTPS.
[b]In this case, the electrode in LE was kept for 14 days.

Conclusion

The electrochemical performance of LTPS in all-solid-state cells using $75Li_2S$-$25P_2S_5$ GC SE was investigated. In a range of 1.5–3.5 V, LTPS showed high first discharge capacity (455 mAh g^{-1}) corresponding with ~10 Li insertion and good cycling performance with capacity retention of 76% at the 25th cycle at 50 mA g^{-1} at 30°C. Further lithiation to 1.0 V leads to a full conversion reaction, as indicated by the evolution of Li_2S, and thus poor reversibility. The LTPS in the conventional LE cells exhibited the similar first discharge capacity as that in the all-solid-state cells, but much poorer cycling performance. ICP-OES measurements revealed that sulfur in the LTPS was dissolved into the LE, and this is strongly believed to be the main cause of poor performance in the LE system. The obtained results highlight the prospect of exploring new electrode materials and reinvestigating previously identified materials that were discarded for conventional LIBs but may be compatible with SEs for all-solid-state batteries.

Acknowledgments

This work was supported by the Energy Efficiency & Resources Program of the Korea Institute of Energy Technology Evaluation and Planning (KETEP) grant funded by the Korea government Ministry of Trade, Industry & Energy (No. 20112010100150) and by by the Future Strategic Fund (1.130019.01) of UNIST (Ulsan National Institute of Science and Technology).

References

1. J. B. Goodenough and Y. Kim, *Chem. Mater.*, **22**, 587 (2010).
2. N. Kamaya, K. Homma, Y. Yamakawa, M. Hirayama, R. Kanno, M. Yonemura, T. Kamiyama, Y. Kato, S. Hama, K. Kawamoto, and A. Mitsui, *Nat. Mater.*, **10**, 682 (2011).
3. T. A. Yersak, H. A. Macpherson, S. C. Kim, V.-D. Le, C. S. Kang, S.-B. Son, Y.-H. Kim, J. E. Trevey, K. H. Oh, C. Stoldt, and S.-H. Lee, *Adv. Energy Mater.*, **3**, 120 (2013).
4. F. Mizuno, A. Hayashi, K. Tadanaga, and M. Tatsumisago, *Adv. Mater.*, **17**, 918 (2005).
5. A. Hayashi, K. Noi, A. Sakuda, and M. Tatsumisago, *Nat. Commun.*, **3**, 856 (2012).
6. A. Sakuda, A. Hayashi, and M. Tatsumisago, *Sci. Report*, **3**, 2261 (2013).
7. R. Kanno and M. Murayama, *J. Electrochem. Soc.*, **148**, A742 (2001).
8. A. Sakuda, A. Hayashi, and M. Tatsumisago, *Chem. Mater.*, **22**, 949 (2010).
9. J. E. Trevey, Y. S. Jung, and S.-H. Lee, *Electrochim. Acta*, **56**, 4243 (2011).
10. A. Sakuda, H. Kitaura, A. Hayashi, K. Tadanaga, and M. Tatsumisago, *J. Electrochem. Soc.*, **156**, A27 (2009).
11. N. Ohta, K. Takada, L. Zhang, R. Ma, M. Osada, and T. Sasaki, *Adv. Mater.*, **18**, 2226 (2006).
12. N. Ohta, K. Takada, I. Sakaguchi, L. Zhang, R. Ma, K. Fukuda, M. Osada, and T. Sasaki, *Electrochem. Commun.*, **9**, 1486 (2007).
13. J. H. Woo, J. E. Trevey, A. S. Cavanagh, Y. S. Choi, S. C. Kim, S. M. George, K. H. Oh, and S.-H. Lee, *J. Electrochem. Soc.*, **159**, A1120 (2012).
14. X. L. Ji, K. T. Lee, and L. F. Nazar, *Nat. Mater.*, **8**, 500 (2009).
15. A. Manthiram, Y. Fu, and Y.-S. Su, *Acc. Chem. Res.*, **46**, 1125 (2013).
16. M. Nagao, A. Hayashi, and M. Tatsumisago, *J. Mater. Chem.*, **22**, 10015 (2012).
17. Z. Lin, Z. Liu, N. J. Dudney, and C. Liang, *ACS Nano*, **7**, 2829 (2013).
18. Y. Kim and J. B. Goodenough, *Electrochem. Commun.*, **10**, 497 (2008).
19. Y. Kim, N. Arumugam, and J. B. Goodenough, *Chem. Mater.*, **20**, 470 (2008).
20. M. S. Whittingham, *Chem. Rev.*, **104**, 4271 (2004).

21. J. E. Trevey, C. R. Stoldt, and S.-H. Lee, *J. Electrochem. Soc.*, **158**, A1282 (2011).
22. Y. S. Jung, K. T. Lee, J. H. Kim, J. Y. Kwon, and S. M. Oh, *Adv. Funct. Mater.*, **18**, 3010 (2008).
23. Y. Oumellal, A. Rougier, G. A. Nazri, J. M. Tarascon, and L. Aymard, *Nat. Mater.*, **7**, 916 (2008).
24. P. Poizot, S. Laruelle, S. Grugeon, L. Dupont, and J.-M. Tarascon, *Nature*, **407**, 496 (2000).
25. J. H. Ku, Y. S. Jung, K. T. Lee, C. H. Kim, and S. M. Oh, *J. Electrochem. Soc.*, **156**, A688 (2009).
26. A. J. Bard and L. R. Faulkner, *Electrochemical Methods: Fundamentals and Applications.* John Wiley & Sons, New York, Ch. 10 (2001).
27. M. Gaberscek, J. Moskon, B. Erjavec, R. Dominko, and J. Jamnik, *Electrochem. Solid-State Lett.*, **11**, A170 (2008).
28. K. Xu, *Chem. Rev.*, **104**, 4303 (2004).
29. Y. S. Jung, P. Lu, A. S. Cavanagh, C. Ban, G.-H. Kim, S.-H. Lee, S. M. George, S. J. Harris, and A. C. Dillon, *Adv. Energy Mater.*, **3**, 213 (2013).
30. M. Nagao, H. Kitaura, A. Hayashi, and M. Tatsumisago, *J. Electrochem. Soc.*, **160**, A819 (2013).